

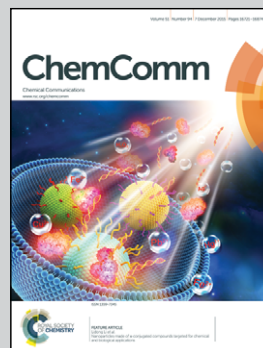


Showcasing research from Qing-Fu Sun's laboratory, Fujian Institute of Research on the Structure of Matter, Fuzhou, China.

A self-assembled Pd_2L_4 cage that selectively encapsulates nitrate

Inspiration of the artwork is from an Ancient Chinese Story, i.e., 'Four Dragons Playing Bead' ('Si Long Xi Zhu' in Chinese). In this picture, the dragon represents the bidentate benzimidazole ligand, with an anthracene spacer. Four dragons twist (right- or left-handed, here right-handed) into a quadruple helicate conformation, defining a concise hydrophobic pocket. The ball represents the nitrate anion, which is selectively encapsulated inside.

As featured in:



See Li-Peng Zhou and Qing-Fu Sun, *Chem. Commun.*, 2015, **51**, 16767.



www.rsc.org/chemcomm

Registered charity number: 207890



Cite this: *Chem. Commun.*, 2015, 51, 16767

Received 31st August 2015,
Accepted 28th September 2015

DOI: 10.1039/c5cc07306e

www.rsc.org/chemcomm

A self-assembled Pd₂L₄ cage that selectively encapsulates nitrate†

Li-Peng Zhou and Qing-Fu Sun*

A M₂L₄ cage with D₄ symmetry was self-assembled from four anthracene-bridged benzimidazole ligands and two Pd^{II} ions. The cage features a concise hydrophobic pocket wrapped up by the anthracene walls with eight hydrogen-bond donors pointing inward, which provide a specific binding site for nitrate, with a binding affinity at least two orders of magnitude higher than all the other anions screened including halide anions, which have a very similar ionic radius and charge density.

Nitrate anion is ubiquitous and important in biology, the environment, and the food industry.¹ Although nitrate is probably benign, it can be reduced to nitrite or other nitric oxides, which react with thiols, amines and amides to form carcinogenic compounds. Other health concerns associated with NO₃[−] metabolism include diabetes, thyroid disorders, respiratory infections and congenital malformations.^{2,3} Therefore, the design of a synthetic host with the capability of selective encapsulation of nitrate is an important task.

Many artificial hosts that can bind nitrate have been documented, including pyrrole,^{4,5} amide,^{6–8} ammonium,^{9,10} urea,¹¹ guanidinium¹² based tripod,¹³ macrocycle,¹⁴ rotaxane,¹⁵ catenane¹⁶ or cage¹⁷ like receptors. Because of the intrinsic properties of nitrate, the reported receptors have several common problems. First of all, large hydration energy and weak basicity of the nitrate anion result in that NO₃[−] is weakly coordinative and it is difficult to form robust hydrogen bonds with the host,^{2,17,18} though hydrogen-bonding interaction plays a crucial role in the anion recognition process.^{19,20} As a result, nitrate anion recognition has been mostly studied in less-polar solvents to favour the hydrogen bonding interactions, and in general poor binding affinity has been reported in polar solvents. Secondly, NO₃[−] has a D_{3h} symmetry with equivalent N–O bonds. Based on the principle of geometrical matching,²⁰

the hydrogen bond donors were limited to a complementary trigonal arrangement in the reported systems.^{15,21} Thirdly, these receptors usually show limited selectivity for NO₃[−].¹⁷ Particularly, due to the negligible difference in ionic radii and charge densities between nitrate and halide anions, it is difficult to selectively recognize nitrate from halide anions.^{13,15} Fourth, the most reported organic hosts generally require tedious multistep synthesis and in most cases give low yield. This means the design of a specific nitrate receptor is still very challenging.

The coordination cages,^{22–28} readily self-assembled from simple organic ligand and metal components, have distinct advantages for the design of new ion receptors. Supramolecular organo-metallic cages avoid tedious synthesis; still they can be regulated easily *via* a rational symmetry consideration regarding the shape of the ligand, the coordination geometry of the metal, and the relative spatial orientation of the ligand and metal components. Although numerous coordination cages have been designed and synthesized for the encapsulation of anions in the literature,^{29–36} to the best of our knowledge, an example where the differentiation between nitrate and halides by the host has never been reported due to the difficulties raised above.

Herein, we succeeded in designing a cationic M₂L₄ cage by a quantitative self-assembly of four anthracene-bridged benzimidazole ligands and two Pd^{II} ions (Fig. 1A). The cage showed a D₄ symmetry, but exhibited excellent capability in the selective encapsulation of nitrate. The binding constant (*K*_{anion}) for the inclusion of NO₃[−] was at least two orders of magnitude higher than all the other anions screened.

Bidentate benzimidazole ligand **1**, with an anthracene spacer, was synthesized in two steps according to an established method.³⁷ After treating ligand **1** (18 μmol) with a half equivalent of Pd(NO₃)₂ (9 μmol) in 700 μL *d*₆-DMSO (dimethyl sulfoxide) for 2 h at 70 °C, the turbid solution turned limpid. The signals of the protons on the complex (**2a**) strongly split and shifted in comparison with those of the free ligand in the ¹H NMR spectrum (Fig. 1B and C). All the signals were assigned carefully based on coupling constants, integrals along with the correlations obtained from the ¹H–¹H COSY spectrum (Fig. S5, ESI†). H_a and H_b of benzimidazole

State Key Laboratory of Structural Chemistry, Fujian Institute of Research on the Structure of Matter, Chinese Academy of Sciences, Fuzhou 350002, P. R. China.

E-mail: qfsun@fjirsm.ac.cn; Fax: +86 591 63173527; Tel: +86 591 63173527

† Electronic supplementary information (ESI) available: Experimental details, supporting figures and tables. CCDC 1048711. For ESI and crystallographic data in CIF or other electronic format see DOI: 10.1039/c5cc07306e



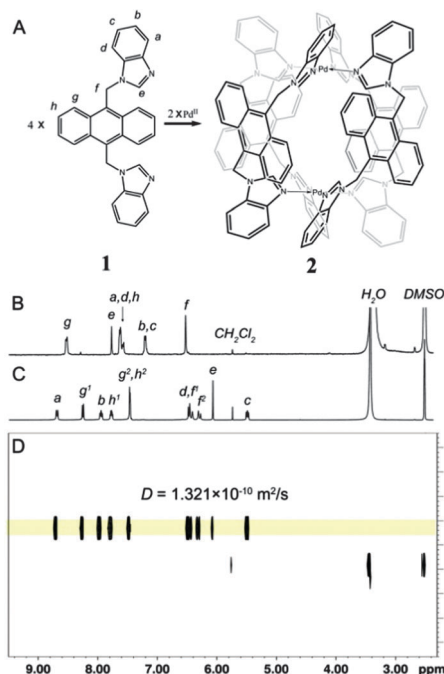


Fig. 1 (A) Self-assembly of complex **2**; the ^1H NMR (400 MHz, d_6 -DMSO, 298 K) spectrum of (B) ligand **1** and (C) complex **2a**; (D) ^1H DOSY spectrum of complex **2a**.

were significantly shifted downfield (from 7.62 ppm and 7.21 ppm to 8.70 ppm and 7.95 ppm, respectively), which is diagnostic for the metal coordination. Diffusion-ordered NMR spectroscopy (DOSY) showed a single product with a single band at the diffusion coefficient $D = 1.321 \times 10^{-10} \text{ m}^2 \text{ s}^{-1}$ ($\log D = -9.879$) (Fig. 1D). The radius of the complex calculated from the D value was 8.42 Å, in accordance with the crystal structures of the complex (see discussion below).

Solid structural confirmation of **2a** was provided by X-ray crystallographic analysis. \ddagger Suitable single crystals were obtained by slow diffusion of 1,4-dioxane vapour into a solution of **2a** in DMSO after about one week. Crystallographic data showed that four ligands in **2a** arranged in a quadruple helicate conformation due to the steric repulsion between the anthracene panels, resulting in a D_4 symmetry of the host framework with inherent P or M helicity (Fig. 2A). Such helical chirality of the host must be maintained in solution to account for the observed diastereomeric splitting for proton $\text{H}_{f,g,h}$ signals on the complex (Fig. 1C).

More interestingly, the four anthracene walls of the ligand wrap up a very concise hydrophobic cavity where all the benzimidazole protons are pointing inward, forming a perfect bind pocket that is occupied by a nitrate anion. Though the nitrate anion is in-plane disordered into four different orientations due to a mismatch of the symmetry, at each orientation its oxygen atoms are involved in at least six hydrogen bonding interactions with the benzimidazole H_e (Fig. 2B), with bonding distances of around 2.124–2.637 Å.

We happened to note that only three out of the four NO_3^- in **2a** could be replaced by BF_4^- after anion exchange by addition of an excess amount of NaBF_4 in a typical anion exchange

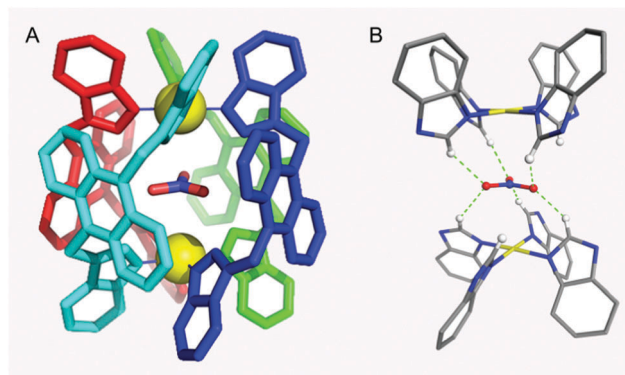


Fig. 2 (A) A perspective view of the crystal structure of **2a** with one encapsulated NO_3^- anion. (Note that the disorder of the central NO_3^- anion was not shown and four ligands were coloured differently to show the quadruple helicate conformation.) (B) Hydrogen bonding interactions (highlighted with green dashed lines) found between the NO_3^- and the benzimidazole ligands. All the other residual molecules were omitted for clarity.

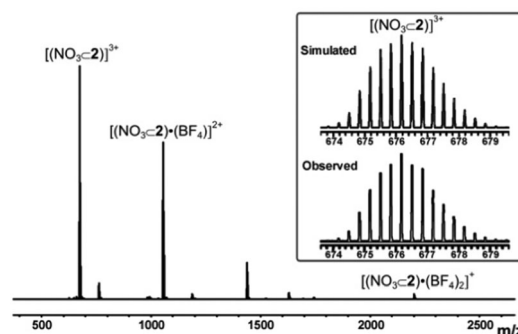


Fig. 3 ESI-Q-TOF mass spectrum of complex $(\text{NO}_3 \subset \mathbf{2}) \cdot (\text{BF}_4)_3$.

procedure, as revealed by ESI-Q-TOF mass spectroscopy (Fig. 3), which showed prominent peaks observed at m/z 2202.5594, 1057.7774, 676.1837, corresponding to the $[(\text{NO}_3 \subset \mathbf{2}) \cdot (\text{BF}_4)_{3-n}]^{n+}$, ($n = 1-3$) respectively. The finely resolved isotopic distribution at each MS signal was also in perfect agreement with the simulated pattern. The IR spectrum also confirmed that the nitrate occupied in the cavity of helicate (Fig. S8, ESI †). This finding inspired us to estimate that cage **2** has a much stronger binding affinity for NO_3^- than BF_4^- .

When $\text{Pd}(\text{CH}_3\text{CN})_4(\text{BF}_4)_2$ was used as the metal source, ^1H and DOSY NMR spectra also suggested the quantitative formation of a similar metal-coordination cage (Fig. S9 and S12, ESI †). However, the ^1H NMR spectrum (complex **2b**) changed dramatically in comparison with that of **2a** (Fig. S23, ESI †). This was the result of the encapsulation of BF_4^- , which was clearly confirmed by the ^{19}F NMR spectrum (Fig. S11, ESI †) and the ESI-Q-TOF mass spectrum (Fig. S14, ESI †). In the ^{19}F NMR spectrum, the signals corresponding to the encapsulated (−145.18 ppm) and the free (−148.24 ppm) BF_4^- anions were both observed. 30 When the bulkier guest BF_4^- , with a radius of 2.27 Å, 38 which is larger than NO_3^- (1.79 Å), was encapsulated *in situ* during the complexation, the cage had to adopt a more twisted configuration. So the difference of δ_{Hf1} with δ_{Hf2} increased, and H_b and H_c are more



downfield shifted. The difference in distortions was also suggested by the coordination conditions. It was necessary to prolong the reaction time or increase the temperature to 110 °C for the formation of **2b**, meaning that it had to overcome a higher energy barrier when BF_4^- was trapped into the cavity.

Though both NO_3^- and BF_4^- could be encapsulated, the cage showed distinct binding affinities between them. After treating **2b** with one equivalent of KNO_3 at 110 °C, the ^1H and ^{19}F NMR spectrum revealed that **2b** converted to **2a** almost quantitatively with the encapsulated BF_4^- released (Fig. S24 and S25, ESI†), which confirmed that cage **2** bound NO_3^- more strongly than BF_4^- .

These observations urged us to make the empty cage **2** for further studies of its specific anion binding properties. We chose $\text{Pd}(\text{PF}_6)_2$ (0.10 M solution in d_6 -DMSO, prepared by reacting PdCl_2 with AgPF_6 in a 1 : 2 ratio at room temperature for 10 h under dark conditions, the AgCl precipitate was then removed by filtration) as the metal source. In contrast to NO_3^- and BF_4^- , PF_6^- with an ionic radius of 2.54 Å³⁸ is significantly larger, and thus should not be encapsulated in the cavity. After treating ligand **1** with $\text{Pd}(\text{PF}_6)_2$ for 2 h at 70 °C, ^1H and DOSY NMR spectra all suggested the quantitative formation of a similar metal-coordination cage **2c** (Fig. S16 and S19, ESI†). The ^{19}F NMR spectrum also confirmed that the PF_6^- was not encapsulated by the cage (Fig. S18, ESI†). However, the ESI-Q-TOF mass spectrum revealed that a chloride ion was trapped into the cavity (Fig. S21, ESI†). The contamination of Cl^- possibly comes from the preparation process of the $\text{Pd}(\text{PF}_6)_2$ solution. This was also confirmed by the anion exchange reactions (Fig. S26 and S27, ESI†) by treating **2b** with 1.1 equivalent of $\text{N}(\text{C}_4\text{H}_9)_4\text{Cl}$ at 110 °C, where new emerging signals attributed to **2c** were observed. The equilibrium constant, calculated by integrating the ^1H NMR spectra, was around 40. The ^{19}F NMR spectrum, showing that BF_4^- was replaced from the cavity by Cl^- , further proved the presence of Cl^- in **2c**. Cl^- , an ionic radius of 1.65 Å, is smaller than NO_3^- and BF_4^- , so **2c** twisted less. This was also supported by the ^1H NMR spectrum, where a smaller diastereomeric splitting between δ_{Hf1} with δ_{Hf2} was observed in comparison to **2a** (Fig. S23, ESI†).

Nevertheless, the presence of Cl^- in the cavity of **2c** had no influence on the study of anion binding properties. Though the binding constants (K_{anion}) could not be obtained, the relative binding ability (*versus* Cl^-) could be exhibited. A series of anions available in the lab were screened for binding ability measurement by treating with cage **2c** (Fig. 4 and Fig. S28, ESI†), from which the equilibrium constants (K , *i.e.*, $K_{\text{anion}}/K_{\text{Cl}}$) (Table 1) for the inclusion of anions, determined by the integration of the characteristic encapsulation signals in the ^1H NMR experiments, were calculated.

For bulky anions, such as CF_3SO_3^- , H_2PO_4^- , and HSO_4^- , no signals referenced to the anion-cage complex were observed. This probably was because they are too bulky to enter the cavity. For Br^- , the equilibrium constant was less than 1, meaning that the binding affinity is weaker than Cl^- . Presumably because the larger Br^- needs host **2** to keep a more high-energy twisted configuration, internal anions were exchanged. Similarly, but more obviously, less exchange for BF_4^- and I^- was observed because of their larger size. As for F^- , conversely, the smaller

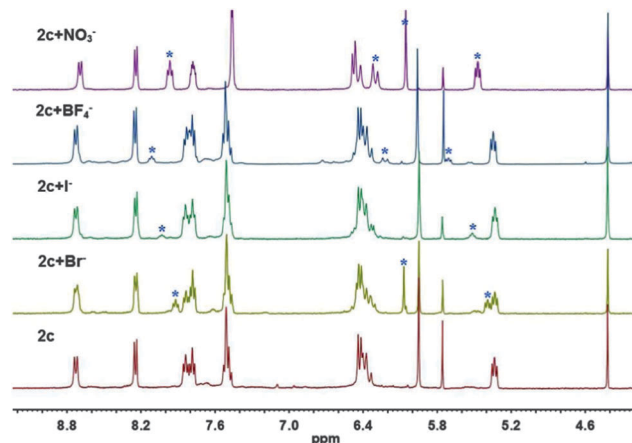


Fig. 4 ^1H NMR (400 MHz, d_6 -DMSO, 298K) spectra showing the encapsulation of different anions by cage **2c**. (1.1 equivalent of anions were added to the solution of **2c** in d_6 -DMSO, * represents the new encapsulation signals.)

Table 1 The equilibrium constants^a of anion exchange of **2c**

$\text{Cl}^- \subset \mathbf{2}(\mathbf{2c}) + \text{Anion} \xrightleftharpoons{K} \text{Anion} \subset \mathbf{2} + \text{Cl}^-$			
Anion	K	Anion	K
NO_3^-	2.56×10^2	NO_2^-	4.12×10^{-3}
Br^-	2.86×10^{-1}	F^-	— ^c
I^-	2.33×10^{-2}	Ac^-	— ^c
BF_4^- ^b	2.5×10^{-2}	CO_3^{2-}	— ^c

^a Determined by the integration of the H_e signals except for the case of BF_4^- where the integration of H_c takes place because of signal overlapping. ^b Determined by the exchange of **2b** with $\text{N}(\text{C}_4\text{H}_9)_4\text{Cl}$. ^c No distinct exchange peaks appeared.

size made its spatial orientation inappropriate, so no distinct peaks appeared. The binding of cage **2** towards Ac^- and CO_3^{2-} was much weaker than Cl^- though they have similar size and geometry compared to nitrate anions.

Notably, for NO_3^- , the equilibrium constant was up to 256, in other words, cage **2** shows two orders of magnitude higher binding affinity toward NO_3^- than Cl^- . Moreover, in the kinetic experiments, the encapsulation of NO_3^- was faster than Br^- (Fig. S29–S31, ESI†). We attributed such a big difference to the presence of maximal hydrogen bonding interactions between the nitrate and the host cage in spite of the mismatching on symmetry. In contrast, the lack of hydrogen bonding weakens this binding between anions and the host even if their symmetries are better matching when single-atom halide anions were placed in the D_4 symmetrical host. Similarly, little exchange for NO_2^- was observed.

In conclusion, a chiral M_2L_4 cage was constructed from the coordination-driven self-assembly of the bidentate ligand **1** and Pd^{II} and showed distinct inclusion behaviour for different anions where unprecedented selective binding toward nitrate was observed.

This work was supported by the National Natural Science Foundation of China (Grant no. 21402201, 21471150, and 21221001), start-up foundation from FJIRSM-CAS, and award of “The Recruitment Program of Global Youth Experts”. We thank Prof. Da-Qiang Yuan (FJIRSM) for his kind assistance with the X-ray data collection.



Notes and references

‡ Crystal data for **2a**: space group C_2 , $a = 13.7980$ (14) Å, $b = 32.546$ (4) Å, $c = 13.7267$ (16) Å, $\alpha = 90^\circ$, $\beta = 100.330$ (10)°, $\gamma = 90^\circ$. $V = 6064.3$ (12) Å³, $Z = 2$, $T = 102$ K. $R_1 = 0.0971$, $wR_2 = 0.2481$, and goodness of fit = 1.075. CCDC 1048711.

- 1 B. Hay, D. Dixon, G. Lumetta, R. Vargas and J. Garza, in *Fundamentals and Applications of Anion Separations*, ed. B. Moyer and R. Singh, Springer, US2004, pp. 43–57.
- 2 M. Strianese, S. Milione, V. Bertolasi and C. Pellecchia, *Inorg. Chem.*, 2013, **52**, 11778–11786.
- 3 O. A. Okunola, P. V. Santacroce and J. T. Davis, *Supramol. Chem.*, 2008, **20**, 169–190.
- 4 J. L. Sessler, D. An, W.-S. Cho, V. Lynch and M. Marquez, *Chem. – Eur. J.*, 2005, **11**, 2001–2011.
- 5 J. L. Sessler, V. Roznyatovskiy, G. D. Pantos, N. E. Borisova, M. D. Reshetova, V. M. Lynch, V. N. Khrustalev and Y. A. Ustynuk, *Org. Lett.*, 2005, **7**, 5277–5280.
- 6 A. P. Bisson, V. M. Lynch, M.-K. C. Monahan and E. V. Anslyn, *Angew. Chem., Int. Ed.*, 1997, **36**, 2340–2342.
- 7 J. M. Mahoney, K. A. Stucker, H. Jiang, I. Carmichael, N. R. Brinkmann, A. M. Beatty, B. C. Noll and B. D. Smith, *J. Am. Chem. Soc.*, 2005, **127**, 2922–2928.
- 8 B. Wu, J. Yang, X. Huang, S. Li, C. Jia, X.-J. Yang, N. Tang and C. Janiak, *Dalton Trans.*, 2011, **40**, 5687–5696.
- 9 S. Mason, T. Clifford, L. Seib, K. Kuczera and K. Bowman-James, *J. Am. Chem. Soc.*, 1998, **120**, 8899–8900.
- 10 L. Cronin, P. A. McGregor, S. Parsons, S. Teat, R. O. Gould, V. A. White, N. J. Long and N. Robertson, *Inorg. Chem.*, 2004, **43**, 8023–8029.
- 11 P. Byrne, G. O. Lloyd, N. Clarke and J. W. Steed, *Angew. Chem., Int. Ed.*, 2008, **47**, 5761–5764.
- 12 P. Blondeau, J. Benet-Buchholz and J. de Mendoza, *New J. Chem.*, 2007, **31**, 736–740.
- 13 M. Işıklan, M. A. Saeed, A. Pramanik, B. M. Wong, F. R. Fronczek and M. A. Hossain, *Cryst. Growth Des.*, 2011, **11**, 959–963.
- 14 R. Herges, A. Dikmans, U. Jana, F. Köhler, P. G. Jones, I. Dix, T. Fricke and B. König, *Eur. J. Org. Chem.*, 2002, 3004–3014.
- 15 M. J. Langton, L. C. Duckworth and P. D. Beer, *Chem. Commun.*, 2013, **49**, 8608–8610.
- 16 M. J. Langton and P. D. Beer, *Chem. Commun.*, 2014, **50**, 8124–8127.
- 17 J. Romański and P. Pitek, *J. Org. Chem.*, 2013, **78**, 4341–4347.
- 18 A. S. Singh and S.-S. Sun, *RSC Adv.*, 2012, **2**, 9502–9510.
- 19 K. Kavallieratos, C. M. Bertao and R. H. Crabtree, *J. Org. Chem.*, 1999, **64**, 1675–1683.
- 20 P. D. Beer and P. A. Gale, *Angew. Chem., Int. Ed.*, 2001, **40**, 486–516.
- 21 A. S. Singh and S.-S. Sun, *J. Org. Chem.*, 2012, **77**, 1880–1890.
- 22 S. M. Biroš, R. M. Yeh and K. N. Raymond, *Angew. Chem., Int. Ed.*, 2008, **47**, 6062–6064.
- 23 M. Yoshizawa, J. K. Klosterman and M. Fujita, *Angew. Chem., Int. Ed.*, 2009, **48**, 3418–3438.
- 24 G. H. Clever, S. Tashiro and M. Shionoya, *J. Am. Chem. Soc.*, 2010, **132**, 9973–9975.
- 25 M. Han, J. Hey, W. Kawamura, D. Stalke, M. Shionoya and G. H. Clever, *Inorg. Chem.*, 2012, **51**, 9574–9576.
- 26 J. J. Henkelis and M. J. Hardie, *Chem. Commun.*, 2015, **51**, 11929–11943.
- 27 N. J. Cookson, J. J. Henkelis, R. J. Ansell, C. W. G. Fishwick, M. J. Hardie and J. Fisher, *Dalton Trans.*, 2014, **43**, 5657–5661.
- 28 J. J. Henkelis, J. Fisher, S. L. Warriner and M. J. Hardie, *Chem. – Eur. J.*, 2014, **20**, 4117–4125.
- 29 R. Custelcean, *Chem. Soc. Rev.*, 2014, **43**, 1813–1824.
- 30 C. Klein, C. Gütz, M. Bogner, F. Topić, K. Rissanen and A. Lützen, *Angew. Chem., Int. Ed.*, 2014, **53**, 3739–3742.
- 31 H. Amouri, L. Mimassi, M. N. Rager, B. E. Mann, C. Guyard-Duhayon and L. Raehm, *Angew. Chem., Int. Ed.*, 2005, **44**, 4543–4546.
- 32 C. Desmarets, F. Poli, X. F. Le Goff, K. Muller and H. Amouri, *Dalton Trans.*, 2009, 10429–10432.
- 33 H. Amouri, C. Desmarets, A. Bettoschi, M. N. Rager, K. Boubekeur, P. Rabu and M. Drillon, *Chem. – Eur. J.*, 2007, **13**, 5401–5407.
- 34 S. Freye, R. Michel, D. Stalke, M. Pawliczek, H. Frauendorf and G. H. Clever, *J. Am. Chem. Soc.*, 2013, **135**, 8476–8479.
- 35 J. K. Clegg, J. Cremers, A. J. Hogben, B. Breiner, M. M. J. Smulders, J. D. Thoburn and J. R. Nitschke, *Chem. Sci.*, 2013, **4**, 68–76.
- 36 I. A. Riddell, M. M. J. Smulders, J. K. Clegg and J. R. Nitschke, *Chem. Commun.*, 2011, **47**, 457–459.
- 37 J.-L. Du, T.-L. Hu, S.-M. Zhang, Y.-F. Zeng and X.-H. Bu, *CrystEngComm*, 2008, **10**, 1866.
- 38 H. Tokuda, K. Hayamizu, K. Ishii, M. A. B. H. Susan and M. Watanabe, *J. Phys. Chem. B*, 2004, **108**, 16593–16600.

